ARTICLE

U-Pb SHRIMP and ^{40}Ar/^{39}Ar constraints on the timing of mineralization in the Paleoproterozoic Caxias orogenic gold deposit, São Luís cratonic fragment, Brazil

Geocronologia do depósito aurífero Paleoproterozoico orogênico do Caxias, fragmento cratônico São Luís, Brasil

Evandro Luiz Klein[1,2]*****, **Colombo Celso Gaeta Tassinari**[3], **Paulo Marcos Vasconcelos**[4]

ABSTRACT: Caxias is an orogenic gold deposit in the São Luís cratonic fragment, which is correlated with the Rhyacian terranes of the West-African Craton. The deposit postdates peak metamorphism (estimated at 2100 ± 15 Ma) and is hosted in a shear zone that cuts across schists of the Aurizona Group (2240 ± 5 Ma) and the Caxias Microtonalite. The emplacement age of the microtonalite, as determined in this work by SHRIMP U-Pb zircon dating, is 2009 ± 11 Ma and represents a late-stage magmatic event in the São Luís cratonic fragment. Older zircon age of 2139 ± 10 Ma is interpreted as due to inheritance from the older granitoid or volcanic suites (magmatic sources?) or to contamination during emplacement. Lead isotope compositions indicate that the Pb incorporated in ore-related pyrite was probably sourced from regional, orogenic calc-alkaline granitoids of *ca.* 2160 Ma. Hydrothermal sericite from Caxias yielded a ^{40}Ar/^{39}Ar plateau age of 1990 ± 30 Ma, which combined with the emplacement age of the Caxias Microtonalite brackets the age of gold mineralization between 2009 ± 11 and 1990 ± 30 Ma.

KEYWORDS: orogenic gold; geochronology; isotope geochemistry.

RESUMO: *Caxias é um depósito de ouro orogênico do fragmento cratônico São Luís, que é correlacionável aos terrenos Riacianos do Cráton Oeste-Africano. O depósito se formou após o metamorfismo regional (estimado em 2100 ± 15 Ma) e está hospedado em zona de cisalhamento que secciona xistos do Grupo Aurizona (2240 ± 5 Ma) e o Microtonalito Caxias. O microtonalito foi aqui datado em 2009 ± 11 Ma, e representa um estágio magmático tardio na evolução do fragmento cratônico São Luís. Cristais de zircão com idades de 2139 ± 10 Ma foram herdados da fonte magmática ou são produto de contaminação durante a intrusão. A composição dos isótopos de chumbo sugere que granitoides de arco de ilhas de ca. 2160 Ma são a fonte provável para o Pb incorporado na pirita relacionada com o minério. Sericita hidrotermal mostra idade ^{40}Ar/^{39}Ar de 1990 ± 30 Ma, que, combinada com a idade de posicionamento do microtonalito hospedeiro, limita o evento mineralizador ao intervalo 2020-1960 Ma.*

PALAVRAS-CHAVE: *ouro orogênico; geocronologia; isótopos.*

[1]CPRM–Geological Survey of Brazil, Belém (PA), Brasil. *E-mail: evandro.klein@cprm.gov.br*

[2]GPGE–Grupo de Pesquisas em Geologia Econômica – Programa de Pós-Graduação em Geologia e Geoquímica; Universidade Federal do Pará - UFPA, Belém (PA), Brasil.

[3]Centro de Pesquisas Geocronológicas, Instituto de Geociências, Universidade de São Paulo - USP, São Paulo (SP), Brasil. *E-mail: ccgtassi@usp.br*

[4]University of Queensland, School of Earth Sciences, Brisbane, Australia. *E-mail: paulo@earth.uq.edu.au*

*Corresponding author

INTRODUCTION

The São Luís cratonic fragment in north-northeastern Brazil hosts one gold mine (Piaba), a few deposits, and a series of showings (Fig. 1) that have been mined by artisanal workers since the 17th century. Caxias (or Touro target, according to Luna Gold Corp) is one of the historically important loci of the artisanal mining, already cited in publications from the beginning of the last century (Moura 1936). More recent works, focused on host rocks and fluid properties, have described the Caxias deposit (sensu lato) as a Paleoproterozoic orogenic gold deposit (Klein *et al.* 2005b and references therein). The attributes of this deposit are similar to those recently described for the more important Piaba deposit (Freitas & Klein 2013, Klein *et al.* in review). In addition, a single-zircon Pb-evaporation age of 1985 ± 4 Ma has been determined for the Caxias Microtonalite, which hosts part of gold mineralization at Caxias (Klein *et al.* 2002). This age has been taken as the maximum age for gold mineralization in this deposit. Geological mapping has been undertaken by the Geological Survey of Brazil in the cratonic area (Klein *et al.* 2008a), followed by high-resolution U-Pb zircon geochronology and whole-rock geochemical studies. These studies have shown that the evolution of the São Luís cratonic fragment took place between about 2240 and 2056 Ma (Fig. 2), comprising rock associations that indicate early arc/back-arc settings (2240 Ma), intensive subduction-related calc-alkaline magmatism in oceanic to continental arc settings (2172 – 2143 Ma), collision-related peraluminous granitic magmatism (2100 Ma), and late- to post-orogenic, evolved volcanic and granitic rocks (*ca.* 2050 Ma) (Klein *et al.* 2005a, 2008b, 2009). The postulated age of the gold-hosting Caxias Microtonalite does not fit in this relatively well-constrained tectonic-geochronological framework, and the role of this rock in the geological evolution of the São Luís cratonic fragments was never understood (Klein *et al.* 2002, 2008a). This fact raised the question about the validity of the published Pb-evaporation age, which can only be considered (Kober 1986) a minimum age for the crystallization of an igneous rock, because one cannot evaluate the degree of discordance of the zircons. Therefore, in this work, the U-Pb sensitive high-resolution ion microprobe (SHRIMP) technique has been used to date zircon crystals from the same sample (here sample EK1) dated by Klein *et al.* (2002), along with crystals from a strongly altered and mineralized sample of the same microtonalite. Dating was preceded by cathodoluminescence (CL) imagery of the zircon crystals to verify possible disturbances or changes in the internal structure of the crystals. In addition, $^{40}Ar/^{39}Ar$ analysis was carried out on hydrothermal sericite and Pb isotope compositions of ore-related pyrite have been determined to investigate the timing of gold deposition in the Caxias deposit.

GEOLOGICAL SETTING

The São Luís cratonic fragment is composed of metavolcano-sedimentary rocks and a variety of granitoids and volcanic rocks (Fig. 1) of different ages and chemical and isotopic signature (Pastana 1995, Costa 2000, Klein *et al.* 2005a, 2008a, 2008b, 2009, Palheta *et al.* 2009). The oldest rocks belong to the metavolcano-sedimentary sequence (2240 ± 5 Ma) of the Aurizona Group, which is interpreted as an island arc–related sequence that was intruded by shallow granophyric rocks at 2214 ± 3 Ma (Piaba unit). This group is subdivided into three formations (Fig. 1): (1) Matará, composed of mafic and ultramafic rocks; (2) Pirocaua, composed of felsic volcanic and pyroclastic rocks; and (3) Ramos, composed of metasedimentary rocks, such as schist, phyllite, chert, and quartzite. These formations record predominantly greenschist facies metamorphic conditions. The batholiths and stocks of juvenile, subduction-related, metaluminous to slightly peraluminous calc-alkaline granitoids of the Tromaí Intrusive Suite developed in an island arc between 2168 ± 4 Ma and 2147 ± 3 Ma and also intruded into the Aurizona Group. The suite is also subdivided into three subunits, named Cavala Tonalite, Bom Jesus Granodiorite, and Areal Granite, from the least to the most evolved. Andesite, dacite, and subordinate basic volcanic rocks of 2164 ± 3 Ma, ascribed to the Serra do Jacaré volcanic unit, formed in a mature arc with minor back-arc component and are coeval with minor calc-alkaline rhyolite, dacite porphyry, and felsic tuffs of 2160 ± 7 Ma of the Rio Diamante Formation. This formation shows very limited Archean inheritance and formed in a continental margin. Peraluminous granites of 2086 – 2091 Ma (Tracuateua Intrusive Suite) crop out in the western portion of the cratonic fragment and are regarded as collision-related rocks. Highly evolved/shoshonitic granites of 2056 – 2076 Ma (Negra Velha Granite) and isolated exposures of felsic volcanic and pyroclastic rocks of 2068 Ma (Rosilha volcanic unit) are the youngest known rocks in the cratonic fragment and are considered to be late- to post-orogenic units. Based on rock association and ages, and geochemical and Nd isotope signatures, these Paleoproterozoic associations have been interpreted as forming part of a Rhyacian orogen that record an accretionary (2240 – 2150 Ma) and a collisional (*ca.* 2100 Ma)
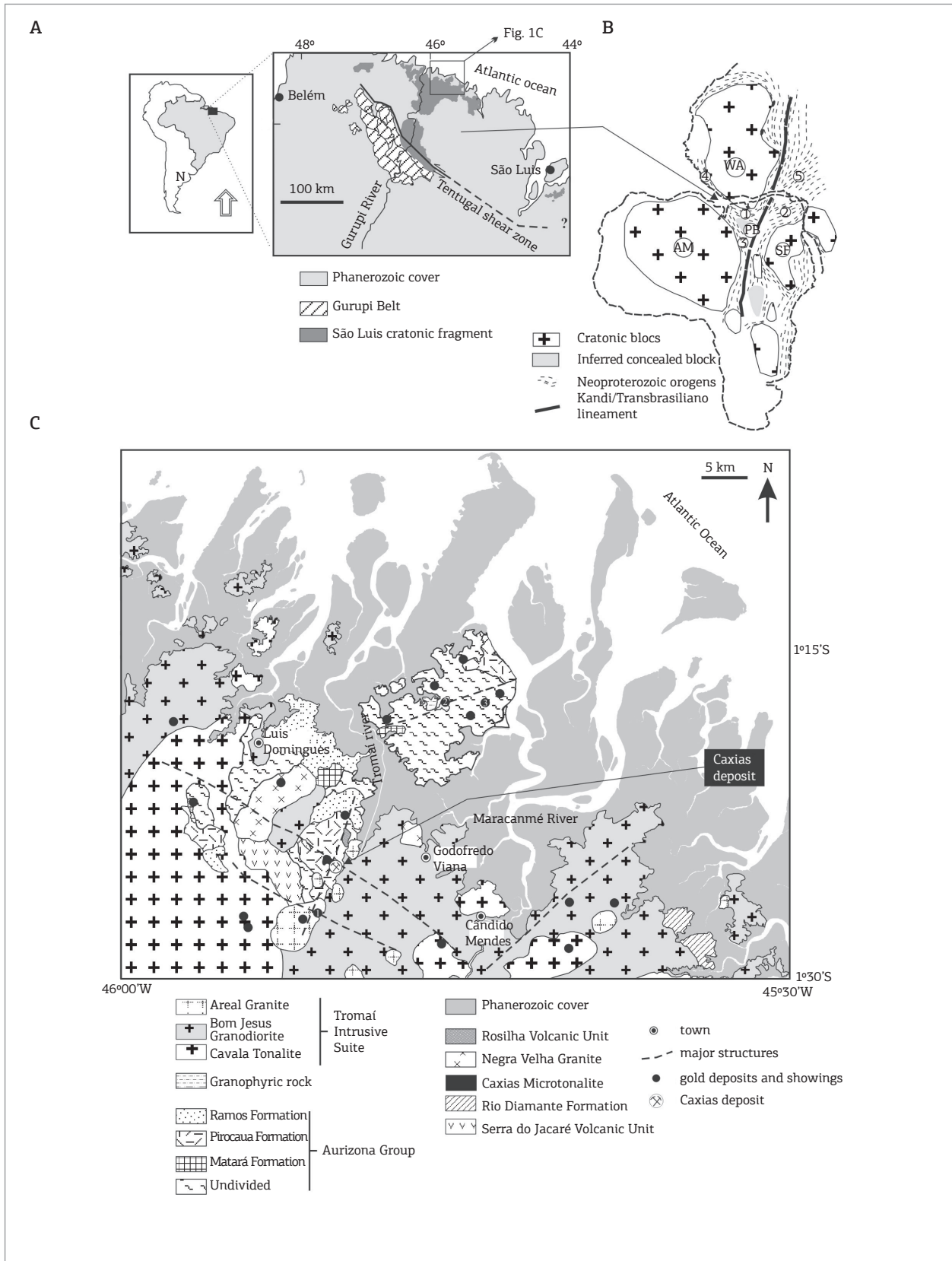
Figure 1. (A) Location map of the exposed portions of the São Luís cratonic fragment and Gurupi Belt. (B) Cartoon not to scale showing the cratons (WA: West African-São Luís Craton; AM: Amazonian Craton; SF: São Francisco Craton; PB: Parnaíba block) and mobile belts (1: Gurupi; 2: Borborema; 3: Araguaia; 4: Rockelide; 5: Dahomeyde) of South America and West Africa. (Modified from Klein and Moura, 2008). (C) Simplified geological map of the northern portion of the São Luís cratonic fragment, with location of Caxias and of the main gold deposits and occurrences (Adapted from Klein *et al.* 2008a). The numbered deposits are those cited in the text. 1: Areal, 2: Piaba, 3: Micote.

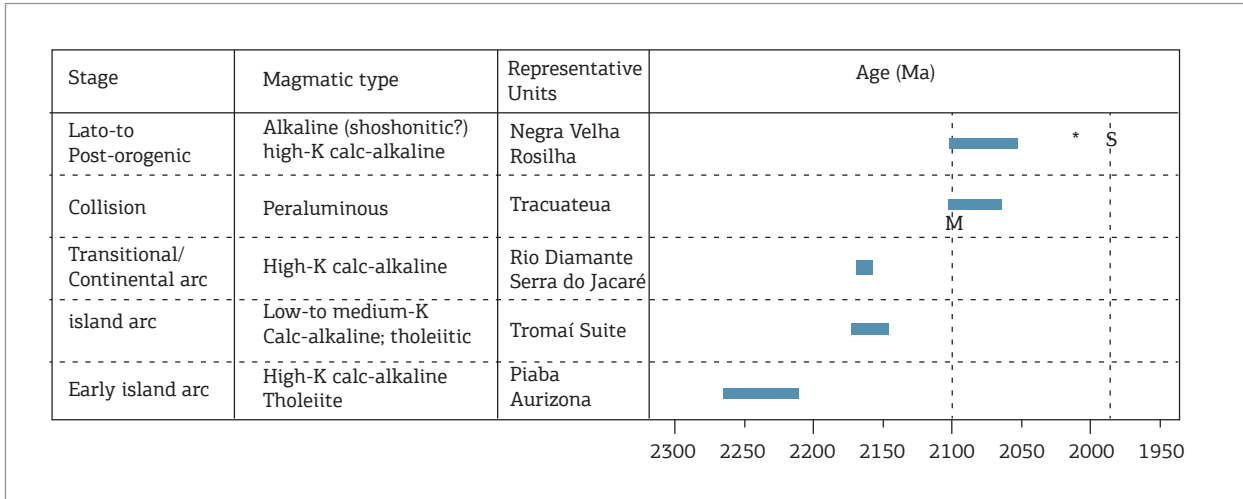| Stage	Magmatic type	Representative Units	Age (Ma)
Lato-to Post-orogenic	Alkaline (shoshonitic?) high-K calc-alkaline	Negra Velha Rosilha	
Collision	Peraluminous	Tracuateua	
Transitional/ Continental arc	High-K calc-alkaline	Rio Diamante Serra do Jacaré	
island arc	Low-to medium-K Calc-alkaline; tholeiitic	Tromaí Suite	
Early island arc	High-K calc-alkaline Tholeiite	Piaba Aurizona	

Figure 2. Known stages of tectonic evolution of the São Luís cratonic fragment with ages of the main magmatic events (references in the text). M: inferred age for the regional metamorphism, based on the emplacement age of strongly-peraluminous granites. s: Hydrothermal sericite $^{40}Ar/^{39}Ar$ age.

phase. Similar evolution has been described for geological units that crop out to the south and form the reworked margin of the São Luís cratonic fragment and the basement of the Gurupi Belt (Klein *et al.* 2012). This scenario also correlates well with what is described for similar successions of the Eburnean-Birimian terranes of the West-African Craton (Klein & Moura, 2008, Perrouty *et al.* 2012, and references therein).

SUMMARY OF THE GEOLOGICAL AND GENETIC ASPECTS OF THE CAXIAS DEPOSIT

Gold mineralization in the Caxias deposit is broadly confined to a right-lateral, N15°E-trending ductile-brittle shear zone (Caxias shear zone; Klein *et al.* 2008a). This shear zone is subvertical and dips >75° both to ESE and WNW, and cuts across pelitic and mafic schists of the Aurizona Group and the Caxias Microtonalite. The mineralized zone is 15 – 30 m thick and is followed at least 300 m along strike (Fig. 3; Klein *et al.* 2002, Klein & Sousa 2012). Recent exploration drilling has intercepted mineralization down to 100 m in depth (www.lunagold.com). Mineralization consists of disseminations in the altered host rocks and is also associated with cm-thick quartz veinlets and quartz stockworks. The ore-related hydrothermal alteration produced mainly chloritization, silicification, and sulfidation of the host rocks and subordinate sericitization and carbonatization (Klein *et al.* 2002, 2008a). Gold occurs as free-milling particles in quartz-chlorite contacts and in pyrite. Higher Au and As contents are associated with higher Ni, Co,

V, and Cr contents, especially in the southern portion of the deposit (Klein *et al.* 2002).

According to Klein *et al.* (2002), the Caxias Microtonalite shows geochemical characteristics similar to those of modern, calc-alkaline, metaluminous, subduction-related granitoids. The igneous shape and the extension of the microtonalite body remain uncertain because of the lack of good and continuous exposures, but it possibly represents a thick dike that intruded the supracrustal rocks of the Aurizona Group (Klein *et al.* 2008a).

Fluid inclusion, stable isotopes, and chlorite chemistry (Klein & Koppe 2000, Klein *et al.* 2000, 2005b) revealed that gold mineralization occurred at 262 – 307°C and 1.6 – 4.6 kbar from a reduced, low-salinity (<5 wt.% NaCl equiv.) aqueous-carbonic fluid, which contains 6 – 45 mol% CO_2 and minor amounts of N_2. This fluid was interpreted to be metamorphic in origin, and the Caxias deposit was included in the class of orogenic gold deposits (Klein *et al.* 2005b, 2008a).

ANALYTICAL PROCEDURES

U-Pb age determinations were carried out at the Centro de Pesquisas Geocronológicas of the University of São Paulo (CPGeo-USP), Brazil. Zircon crystals were separated using conventional heavy liquid and magnetic techniques. The crystals were further mounted, together with the TEMORA-2 standard (Black *et al.* 2004), in epoxy and polished to expose the interior of the grains. After coating with Au, the polished mounts were comprehensively examined with a FEI Quanta 250 scanning electron microscope equipped with secondary-electron
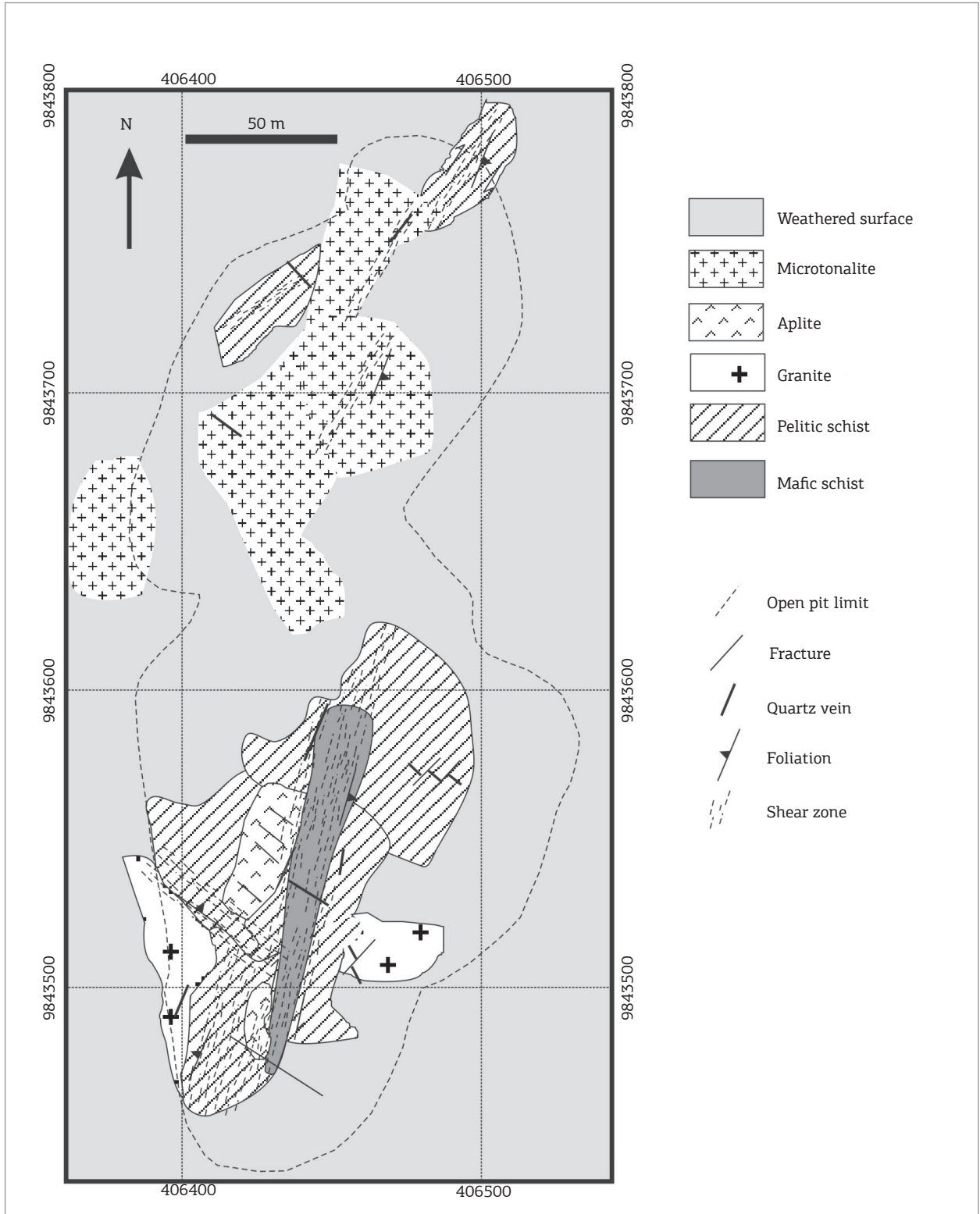
Figure 3. Simplified geological map of the Caxias gold deposit (Adapted from Klein and Sousa, 2012).

and CL detectors at IGc-CPGeo-USP; the most common conditions used in CL analysis were as follows: 60 µA emission current, 15.0 kV accelerating voltage, 7 µm beam diameter, 200 µs acquisition time, and a resolution of 1024 × 884. The same mounts were afterwards analyzed by the U-Pb isotopic technique using a

SHRIMP-IIe machine following the analytical procedures presented by Williams (1998). Correction for common Pb was made based on the basis of the ^{204}Pb measured, and the typical error for the ^{206}Pb/^{238}U ratio is less than 2%; uranium abundance and U/Pb ratios were calibrated against the TEMORA standard, and the ages were calculated using Isoplot® version 3.0 software application (Ludwig 2003). Errors are reported as 1σ deviations and ages have been calculated at the 95% confidence level.

Ar isotope ratios were obtained at the University of Queensland Argon Geochronology in Earth Sciences laboratory, Brisbane, Australia. The crushed material was cleaned in an ultrasonic bath for at least 1 and 1.5 h, respectively, with distilled water and ethanol and then dried. Twenty to fifty grains (0.5 – 2 mm in size) were hand-picked from the cleaned material using a binocular microscope. From each sample, 5 – 10 grains were placed into aluminum irradiation disks along with Fish Canyon sanidine standards (28.201 ± 0.046 Ma; Kuiper *et al.* 2008). The irradiation disks were closed with aluminum covers, wrapped in aluminum foil, and vacuum heat sealed into quartz vials. The quartz vials were irradiated for 14 h at the B-1 CLICIT facility at the Radiation Center, Oregon State University, USA. After a decay period, one to three grains from each sample were analyzed by incremental laser ^{40}Ar/^{39}Ar step heating following procedures detailed by Vasconcelos *et al.* (2002).

Pb isotope analyses were carried out at the Laboratório de Geologia Isotópica – Para-Iso – of the Universidade Federal do Pará, in Belém, Brazil. The experimental procedure used 20 – 50 mg of pyrite for total dissolution and about 250 mg sulfide mineral for the step-leaching technique. The mineral concentrates were washed with distilled water and HCl, and sample dissolution was obtained by using a combination of HCl, HNO$_3$, and HBr (Rodrigues 1992). The Pb separation was done in Teflon columns containing DOWEX AG 1 × 8 (200 – 400 mesh) resin through sequential addition of HBr and HCl. Pb was deposited on Re filaments with a combination of HCl and H$_3$PO$_4$, and the isotope composition was obtained with VG ISOMASS 54E mass spectrometers. For model age calculation, the Isoplot software (Ludwig 2003) was used.

GEOCHRONOLOGY AND ISOTOPE GEOLOGY

U-Pb SHRIMP results

Zircon crystals from weakly altered and altered samples of the Caxias Microtonalite have been analyzed using the U-Pb SHRIMP technique. The analytical results are presented in Tab. 1 and CL images with location of analytical points are shown in Fig. 4.

Sample EK1 is from the least altered microtonalite. Most zircon crystals are 100 – 110 μm long. Some crystals are, in fact, fragments of larger grains, and some show corroded rims and embayments. Most crystals show growth zoning; a few have bright rims in CL images and some show disturbance of the primary magmatic structure (Fig. 4A). Several analyses are highly discordant and/or with high U contents and were not used in age calculations. Considering only the fourteen concordant and slightly discordant (≤7%) spots, two groups of ^{207}Pb/^{206}Pb apparent ages are observed (Fig. 5A). The eight older spots yielded a concordia age of 2139 ± 10 Ma (MSWD = 0.60), whereas the six younger spots returned an age of 2009 ± 11 Ma (MSWD = 0.28).

Only ten zircon crystals were obtained from sample EK2 (altered microtonalite, used to verify possible influence of the hydrothermal fluid on zircon). The smallest crystals are 45 – 70 μm long, whereas the largest crystals are about 110 mm in length. The crystals show external morphology and some internal structures indicating igneous crystallization. The low luminescence in CL images (Fig. 4B) of these crystals indicates normal to high uranium contents. Some crystals show patchily zoned interiors, which might indicate crystallization at depth (e.g. Vavra 1994). Some other crystals show irregular internal portions, and their low luminescence in CL images is ascribed to high uranium contents. The isotopic ratios of individual spots show moderate to high variation and moderate to high discordance, and all ratios plot along a discordia line (Fig. 5B) that define an upper intercept age of 2155 ± 26 Ma (MSWD = 0.77). Despite the large error, this age overlaps with the age yielded by the older concordant group of sample EK1.

Pb isotope results

The step-leaching technique was applied to ore-related pyrite to place constraints on the deposition age and on the source of Pb of the ore. The results (Tab. 2) show that the isotopic ratios are highly radiogenic. A regression through the analytical points produced a straight line (Fig. 6) that corresponds to ^{207}Pb/^{204}Pb *versus.* ^{206}Pb/^{204}Pb age of 2170 ± 29 Ma (MSWD = 1.6). This line intercepts the Pb evolution curve of Stacey and Kramers (1975) at 2151 Ma and 43 Ma (i.e., close to 0 Ma).

^{40}Ar/^{39}Ar results

Two sericite grains extracted from a hydrothermal zone of the altered microtonalite were analyzed (Tab. 3).

Table 1. Summary of zircon U-Pb SHRIMP data

Spot	% Comm 206Pb	U (ppm)	Th (ppm)	232Th /238U	206Pb /238U Age (Ma)c	1s	207Pb /206Pb Age (Ma)c	1s	% Discord	207Pb /206Pb*	% Error	207Pb /235Pb*	% Error	206Pb /238Pb*	% Error	Error correl
Sample								EK1								
1.1**	0.21	251	110	0.45	2235.5	66.7	2152	10	-4	0.1340	0.6	7.66	3.6	0.4145	3.5	0.991
2.1*	2.77	116	110	0.98	2043.8	64.8	2003	58	-2	0.1232	3.3	6.34	5.0	0.3731	3.7	0.784
3.1	0.84	222	125	0.58	1513.5	49.6	1960	23	29	0.1202	1.3	4.39	3.9	0.2646	3.7	0.702
4.1*	0.10	207	239	1.19	1936.6	59.5	2020	12	4	0.1244	0.6	6.01	3.6	0.3504	3.6	0.987
4.2*	0.12	312	147	0.49	2000.7	60.7	1993	10	0	0.1225	0.6	6.15	3.6	0.3639	3.5	0.990
5.1**	0.49	227	135	0.61	1981.5	60.3	2129	13	7	0.1323	0.8	6.56	3.6	0.3598	3.5	0.906
6.1**	0.07	63	19	0.30	2193.1	67.8	2126	19	-3	0.1321	1.1	7.38	3.8	0.4052	3.6	0.963
6.2*	0.23	63	19	0.31	2152.6	67.1	2132	22	-1	0.1326	1.2	7.25	3.9	0.3964	3.7	0.958
7.1**	2.55	289	66	0.23	1979.7	63.8	2044	58	3	0.1261	3.3	6.25	5.0	0.3595	3.7	0.904
8.1*	0.37	401	130	0.33	1965.5	59.8	2006	11	2	0.1234	0.6	6.06	3.6	0.3565	3.5	0.991
8.2**	0.00	321	74	0.24	2095.1	63.1	2023	8	-3	0.1246	0.5	6.60	3.6	0.3840	3.5	0.991
9.1	1.67	167	40	0.25	1430.4	47.7	2030	37	42	0.1251	2.1	4.28	4.3	0.2484	3.7	0.789
9.2	1.07	896	105	0.12	807.9	27.2	1381	42	71	0.0879	2.2	1.62	4.2	0.1335	3.6	0.891
10.1*	0.21	281	109	0.40	2151.6	64.6	2145	10	0	0.1335	0.6	7.29	3.6	0.3962	3.5	0.990
11.1**	1.96	1053	397	0.39	2096.1	62.8	2158	29	3	0.1346	1.7	7.13	3.9	0.3842	3.5	0.911
12.1*	0.70	147	58	0.40	2094.7	64.0	2108	18	1	0.1308	1.0	6.92	3.7	0.3840	3.6	0.975
12.2	5.07	882	205	0.24	802.8	26.6	1551	119	93	0.0961	6.3	1.76	7.3	0.1326	3.5	0.509
13.1*	0.46	381	81	0.22	2187.7	65.4	2146	11	-2	0.1336	0.6	7.44	3.6	0.4041	3.5	0.994
Sample								EK2								
1.1	10.88	1317	228	0.18	839.2	29.0	1311	336	56	0.0848	17.3	1.63	17.7	0.1390	3.7	0.372
1.2	0.90	622	295	0.49	1920.8	58.4	2141	19	11	0.1332	1.1	6.38	3.7	0.3471	3.5	0.973
2.1	1.10	250	106	0.44	1967.0	59.9	2107	23	7	0.1306	1.3	6.43	3.8	0.3568	3.5	0.828
3.1	3.08	495	183	0.38	1469.5	46.3	1952	56	33	0.1197	3.2	4.23	4.7	0.2560	3.5	0.896
4.1	0.00	181	88	0.50	2298.1	68.6	2163	10	-6	0.1349	0.6	7.97	3.6	0.4283	3.6	0.981
5.1	10.93	957	296	0.32	902.6	30.4	1662	253	84	0.1021	13.6	2.12	14.1	0.1503	3.6	0.187
6.1	2.84	292	225	0.80	1833.9	56.5	2092	47	14	0.1296	2.7	5.88	4.4	0.3291	3.5	0.750
7.1	21.06	792	305	0.40	889.3	32.6	1946	439	119	0.1193	24.5	2.43	24.8	0.1479	3.9	0.058
8.1	2.31	525	94	0.19	1364.6	43.4	1902	44	39	0.1164	2.4	3.78	4.3	0.2358	3.5	0.837
9.1	13.42	1175	384	0.34	1050.6	35.1	1885	262	79	0.1153	14.6	2.81	15.0	0.1770	3.6	0.199
10.1	10.82	1047	687	0.68	706.7	24.0	1504	269	113	0.0938	14.2	1.50	14.7	0.1159	3.6	0.236
10.2	11.66	870	689	0.82	750.8	25.7	1471	303	96	0.0922	16.0	1.57	16.4	0.1235	3.6	0.875

c204Pb corrected.
*and **spots used for age calculations of sample EK1 (older and younger populations, respectively); for sample EK2 all spots were used.

They produced plateau ages of 1980 ± 20 and 1988 ± 19 Ma, defined by ~50 and 80% of total 39Ar released, respectively. The two plateau ages are compatible at the 2σ confidence level. The age spectra (Fig. 7) indicate multiple gas reservoirs, with a medium- to high-temperature reservoir indicated by the plateau steps and a moderate
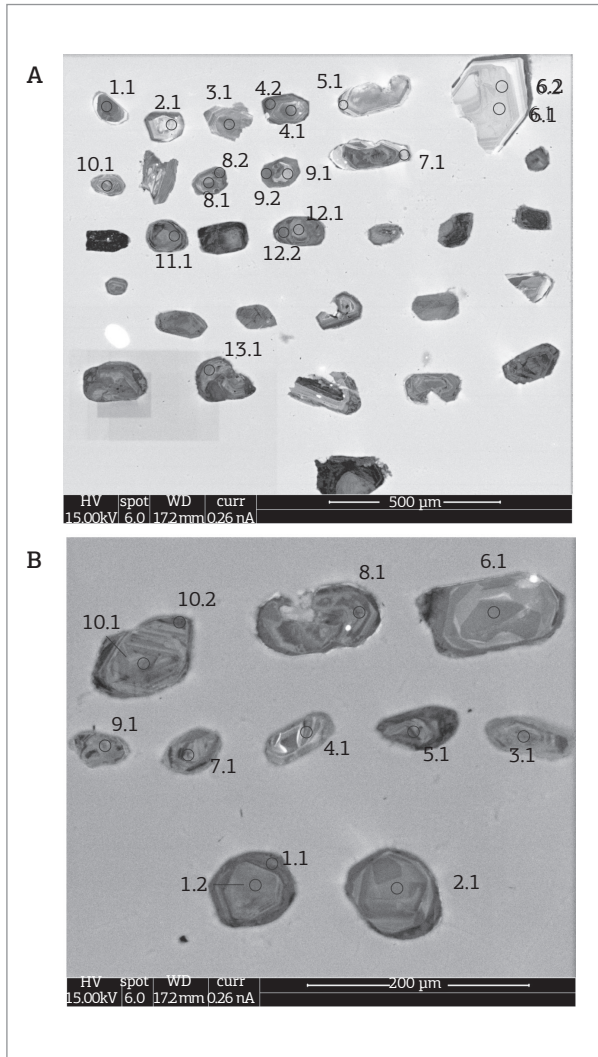
Figure 4. Cathodoluminescence images of zircon crystals from the unaltered (A) and altered (B) samples of the Caxias Microtonalite.

Figure 5. U-Pb Concordia diagrams for the unaltered (A) and altered (B) samples of the Caxias Microtonalite.

K/Ca ratio. In both grains, the highest temperature steps show a decrease in the K/Ca ratio corresponding to an increase in age of the steps. The decrease in age of the lower temperature steps is probably due to alteration or re-heating and Ar loss. Combining the plateau steps of the two grains yields a mean weighted age of 1990 ± 30 Ma is obtained, which is compatible at the 2σ level with the ages given by the plateaus. This combination is the best estimate for the minimum age for the sericite sample.

DISCUSSION

Age of the Caxias Microtonalite

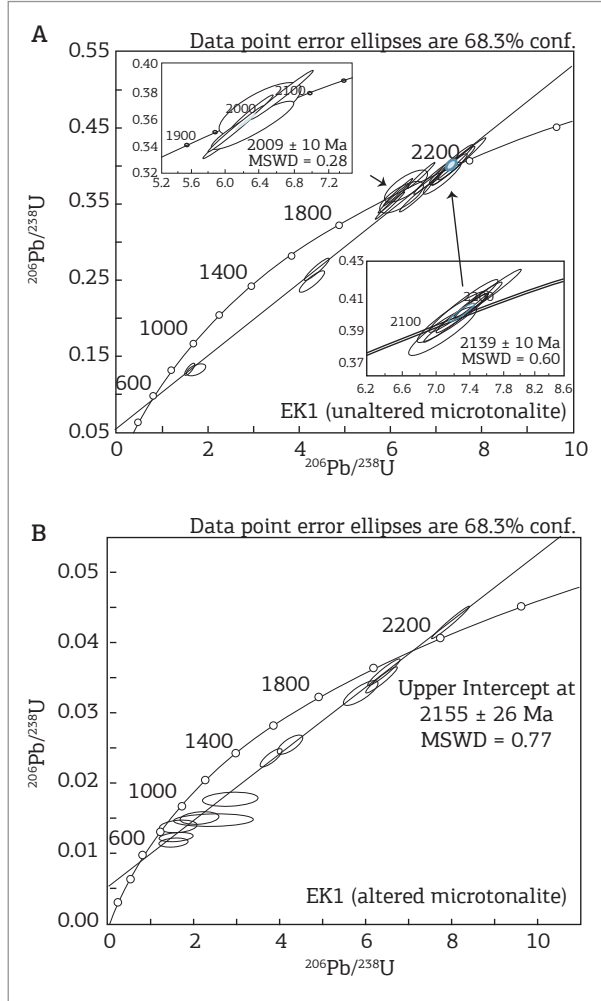Two concordant U-Pb zircon ages, 2139 ± 10 and 2009 ± 11 Ma, were obtained from sample EK1, and a discordia was obtained for sample EK2, which, despite the large uncertainty (2155 ± 26 Ma), overlaps with the older age from sample EK1. Two explanations are envisaged for the data. (1) The older concordant age represents the timing of emplacement of the Caxias Microtonalite, and the younger concordant age reflects postmagmatic Pb loss induced by hydrothermal alteration and mineralization. If so, one will expect a similar behavior for the altered sample EK2, which is not the case. The moderate to high discordance of the zircons from the altered sample hinders a better evaluation of this case. (2) The older zircons are inherited and the younger zircons define the crystallization age of the microtonalite. The patchy zoning of some crystals in sample EK2 indicating crystallization at depth might favor this hypothesis, which is preferred here. It is noteworthy that many of the analyzed spots are in the cores of zircon grains rather than in the outer zoned areas that are more likely

Table 2. Pb isotope results

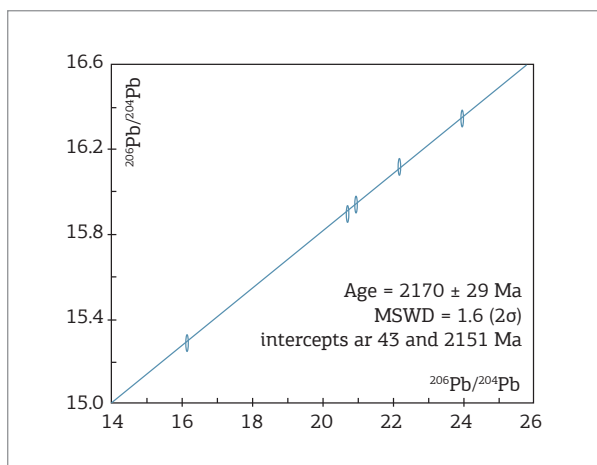| Leaching step	$^{206}Pb/^{204}Pb$	2s	$^{207}Pb/^{204}Pb$	2s	$^{208}Pb/^{204}Pb$	2s	$^{207}Pb/^{206}Pb$
1	24.006	0.015	16.347	0.015	42.208	0.050	0.6800
2	22.203	0.014	16.121	0.015	41.119	0.050	0.7252
3	20.952	0.013	15.940	0.015	45.060	0.050	0.7599
4	20.714	0.014	15.900	0.016	45.660	0.060	0.7667
5	16.163	0.010	15.290	0.014	35.680	0.040	0.9451

Figure 6. $^{207}Pb/^{204}Pb$ vs. $^{206}Pb/^{204}Pb$ diagram for ore-related pyrite of the Caxias gold deposit.

to give the age of igneous crystallization. The inheritance might have been acquired from the magmatic sources by contamination during ascent and emplacement. The inherited ages of 2140 – 2150 Ma are consistent with the Tromaí Suite or Serra do Jacaré volcanic unit as potential sources. The partial overprinting of the internal structure of some analyzed zircons (Fig. 4) might have been produced by the hydrothermal event associated with gold deposition.

Age of gold mineralization

Orogenic gold deposits may be produced at any time during the development of an orogen, but most deposits form 20 – 100 Ma after formation of the host rocks and show post-metamorphic, postcollision, and syn- to late-tectonic timing (Groves *et al.* 2003, Goldfarb *et al.* 2005). Although the structural and metamorphic evolution of the São Luís cratonic fragment is not fully understood (these events have not been dated yet), the known magmatic evolution of this cratonic area is relatively well constrained, from 2240 to 2056 Ma. Rocks

of syncollisional aspect (strongly peraluminous two-mica granites) were emplaced at 2100 ± 15 Ma, and the youngest known magmatic rocks (Negra Velha Granite and Rosilha volcanic unit) formed at about 2056 – 2076 Ma (Fig. 2) and do not show evidence of metamorphism or significant ductile deformation.

Geological evidence shows that gold mineralization in the São Luís cratonic fragment as a whole postdates regional metamorphism, which is inferred from the timing of emplacement of the peraluminous granitoids at 2100 ± 15 Ma (Klein *et al.* 2008a, 2012).

Gold mineralization at Caxias postdates the intrusion of the Caxias Microtonalite and is, therefore, younger than 2009 ± 11 Ma. Despite the good alignment of the analytical points obtained by the step-leaching technique, a large analytical error is associated with the Pb–Pb isochron age of pyrite (2170 ± 29 Ma). This isochron intercepts the model growth curve of Stacey and Kramers (1975) at 2151 and 43 Ma. The lower intercept indicates that Pb loss occurred only in recent times. The upper intercept age is, within error, similar to the isochron age and might suggest that the Pb incorporated in pyrite has evolved according to, or close to, the model curve. The upper intercept age is also very similar to the age of granitoids of the Tromaí Intrusive Suite, which is the predominant exposed unit in the region. This upper intercept age is thus interpreted as the age of the source of the Pb incorporated in pyrite.

The integrated $^{40}Ar/^{39}Ar$ age of 1990 ± 30 Ma of sericite is thought to date the hydrothermal system in which the mineral has formed. This age is similar to argon ages found in other deposits and showings of the São Luís cratonic fragment (1920 – 1980 Ma), such as Areal, Micote (Klein *et al.* 2008a), and Piaba (Klein *et al.* in review). Hence, gold mineralization at Caxias must have occurred between 2009 ± 11 Ma and 1990 ± 30 Ma, that is, late in the geological evolution of the São Luís cratonic fragment.

Table 3. Ar data on hydrothermal sericite

| run_ID	$^{36}Ar/^{39}Ar$	±	$^{37}Ar/^{39}Ar$	±	Ca/K	±	$^{38}Ar/^{39}Ar$	±	$^{40}Ar/^{39}Ar$	±	$^{40}Ar*/^{39}Ar$	±	Ar* (%)	±	Age (Ma)	±
4377-01A	0.1305	0.0061	1.49	0.42	2.92	0.83	0.0357	0.0049	562.00	15.00	524.00	14.00	93.09	0.34	1922.00	32.00
4377-01B	0.0265	0.0009	3.99	0.10	7.82	0.19	0.0176	0.0011	184.40	1.50	177.30	1.50	95.88	0.22	896.80	6.00
4377-01C	0.0191	0.0012	12.46	0.22	24.41	0.44	0.0164	0.0015	393.00	4.50	391.70	4.60	98.80	0.16	1597.00	12.00
4377-01D	0.0129	0.0010	11.63	0.20	22.80	0.39	0.0149	0.0012	424.90	4.90	425.40	5.00	99.31	0.15	1686.00	13.00
4377-01E	0.0087	0.0009	2.64	0.08	5.17	0.16	0.0062	0.0012	567.80	4.90	566.50	4.90	99.58	0.16	2017.00	10.00
4377-01F	0.0057	0.0006	0.19	0.04	0.37	0.08	0.0110	0.0007	566.70	4.70	565.10	4.70	99.70	0.12	2014.00	10.00
4377-01H	0.0044	0.0006	0.23	0.05	0.44	0.09	0.0133	0.0008	557.30	4.80	556.10	4.80	99.77	0.12	1994.00	10.00
4377-01I	0.0029	0.0006	0.23	0.05	0.44	0.09	0.0135	0.0008	544.40	5.20	543.60	5.20	99.85	0.14	1967.00	11.00
4377-01J	0.0011	0.0012	0.24	0.07	0.46	0.13	0.0109	0.0012	539.00	4.80	538.80	4.80	99.94	0.18	1956.00	11.00
4377-01K	0.0048	0.0011	0.36	0.09	0.71	0.17	0.0168	0.0015	548.30	5.40	547.00	5.40	99.75	0.21	1974.00	12.00
4377-01L	0.0072	0.0012	0.32	0.09	0.62	0.18	0.0152	0.0013	559.10	6.00	557.10	6.10	99.62	0.20	1996.00	13.00
4377-01M	0.0079	0.0009	0.70	0.08	1.36	0.16	0.0142	0.0011	560.50	5.60	558.40	5.60	99.59	0.13	1999.00	12.00
4377-01N	0.0130	0.0012	1.06	0.11	2.08	0.22	0.0183	0.0015	575.50	7.00	572.10	7.00	99.34	0.14	2029.00	15.00
4377-01O	0.0183	0.0018	1.70	0.16	3.33	0.31	0.0191	0.0020	582.40	9.10	577.70	9.10	99.08	0.17	2040.00	19.00
4377-01P	0.0152	0.0030	1.07	0.29	2.10	0.56	0.0141	0.0035	604.00	14.00	600.00	14.00	99.26	0.23	2088.00	30.00
4377-01Q	0.0182	0.0016	1.41	0.13	2.76	0.26	0.0195	0.0019	674.80	9.20	670.10	9.20	99.21	0.14	2226.00	18.00
4377-01R	0.0183	0.0026	1.69	0.20	3.30	0.39	0.0209	0.0026	681.00	14.00	677.00	14.00	99.22	0.18	2239.00	26.00
4377-02A	0.0699	0.0053	0.91	0.47	1.78	0.91	0.0249	0.0055	230.30	7.30	209.60	6.90	90.97	0.67	1022.00	26.00
4377-02B	0.0167	0.0018	7.06	0.25	13.83	0.48	0.0148	0.0019	321.60	5.20	318.70	5.20	98.62	0.24	1388.00	16.00
4377-02C	0.0064	0.0016	10.53	0.25	20.64	0.49	0.0150	0.0016	450.80	6.50	453.10	6.60	99.76	0.18	1756.00	16.00
4377-02D	0.0055	0.0012	1.35	0.11	2.65	0.21	0.0116	0.0013	558.60	6.90	557.60	6.90	99.73	0.16	1997.00	15.00
4377-02E	0.0042	0.0012	0.19	0.09	0.37	0.18	0.0137	0.0013	563.50	5.90	562.40	6.00	99.78	0.16	2008.00	13.00
4377-02F	0.0030	0.0010	-0.02	0.08	-0.04	0.15	0.0132	0.0012	564.30	5.10	563.40	5.10	99.84	0.12	2010.00	11.00
4377-02G	0.0033	0.0010	-0.04	0.07	-0.08	0.13	0.0120	0.0011	551.60	5.20	550.60	5.20	99.82	0.13	1982.00	11.00
4377-02H	0.0036	0.0008	0.07	0.06	0.13	0.11	0.0139	0.0009	552.00	4.30	551.00	4.30	99.81	0.11	1983.00	9.40
4377-02I	0.0044	0.0007	0.03	0.07	0.05	0.14	0.0139	0.0010	552.50	5.30	551.20	5.30	99.76	0.20	1983.00	12.00
4377-02J	0.0036	0.0009	0.01	0.08	0.01	0.15	0.0141	0.0010	549.70	5.00	548.60	5.10	99.80	0.18	1978.00	11.00
4377-02K	0.0038	0.0010	-0.02	0.07	-0.03	0.13	0.0140	0.0012	546.10	5.30	544.90	5.40	99.79	0.14	1970.00	12.00
4377-02L	0.0040	0.0009	0.31	0.08	0.60	0.16	0.0150	0.0010	554.20	5.50	553.20	5.50	99.79	0.15	1988.00	12.00
4377-02M	0.0057	0.0011	0.33	0.09	0.65	0.17	0.0147	0.0012	550.90	5.70	549.30	5.70	99.70	0.14	1979.00	13.00
4377-02N	0.0102	0.0024	0.78	0.18	1.52	0.35	0.0191	0.0027	572.00	12.00	570.00	12.00	99.48	0.18	2023.00	25.00
4377-02O	0.0090	0.0027	0.52	0.27	1.02	0.52	0.0225	0.0036	613.00	15.00	610.00	15.00	99.57	0.26	2108.00	30.00
4377-02P	0.0068	0.0017	0.48	0.16	0.95	0.32	0.0202	0.0020	616.00	11.00	614.00	11.00	99.68	0.22	2116.00	21.00
4377-02Q	0.0050	0.0028	0.74	0.28	1.45	0.55	0.0256	0.0034	600.00	14.00	598.00	14.00	99.76	0.22	2084.00	29.00
4377-02R	0.0052	0.0031	1.00	0.30	1.97	0.58	0.0201	0.0034	664.00	16.00	663.00	17.00	99.78	0.23	2213.00	32.00

*Errors at 2-sigma level.
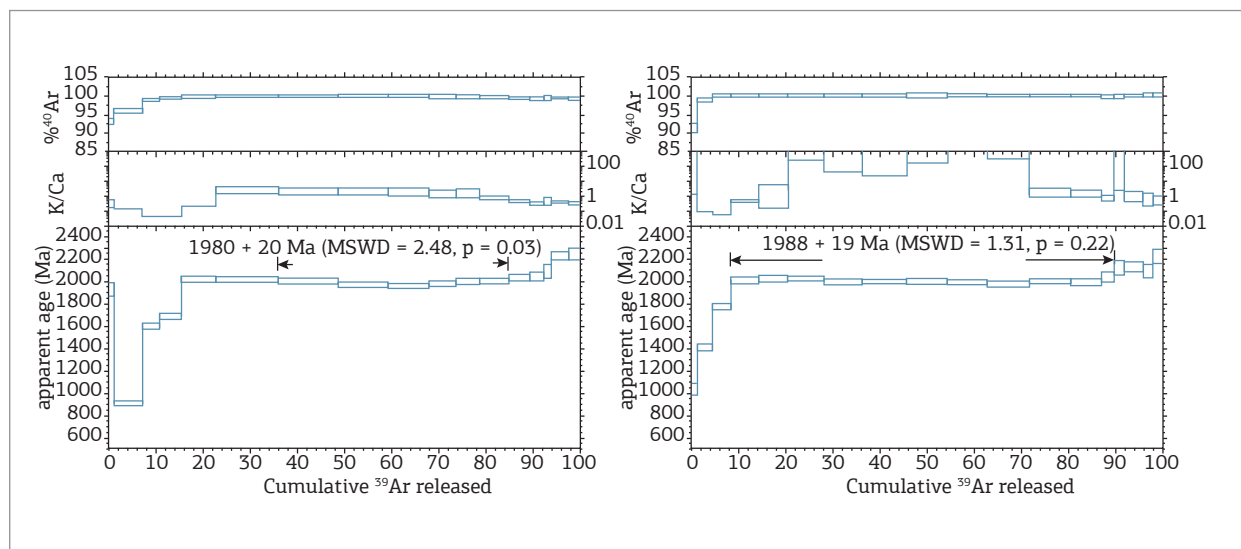
Figure 7. $^{40}Ar/^{39}Ar$ age spectra as a function of %^{39}Ar released. Plateau ages calculated at the 2-sigma level.

CONCLUSIONS

New geochronological and isotopic data obtained in rocks and hydrothermal minerals from the orogenic Caxias gold deposit allowed us to draw the following conclusions:

■ The emplacement age of the gold hosting Caxias Microtonalite is 2009 ± 11 Ma. This is the youngest magmatic age known in the São Luís cratonic fragment so far. Older zircons dated at *ca.* 2.15 Ga in two samples are interpreted as inherited from the magmatic source or contamination of the magma during emplacement.

■ Pb isotopes suggest that the Pb incorporated in ore-related pyrite was sourced from regional calc-alkaline granitoids of *ca.* 2160 Ma, consistent with our interpretation of inherited zircon.

■ The timing of gold mineralization at Caxias is constrained by the emplacement age of the Caxias Microtonalite and the $^{40}Ar/^{39}Ar$ age of hydrothermal sericite and took place between 2009 ± 11 Ma and 1990 ± 30 Ma.

ACKNOWLEDGMENTS

REFERENCES

Black L.P., Kamo S.L., Allen C.M., Davis D.W., Aleinikoff J.N., Valley J.W., Mundil R., Campbell I.H., Korsch R.J., Williams I.S., Foudoulis C. 2004. Improved $^{206}Pb/^{238}U$ microprobe geochronology by the monitoring of a trace-element-related matrix effect; SHRIMP, ID-TIMS, ELA-ICP-MS and oxygen isotope documentation for a series of zircon standards. *Chemical Geology*, **205**:115-140.

Costa J.L. 2000. *Programa Levantamentos Geológicos Básicos do Brasil. Programa Grande Carajás. Castanhal, Folha SA.23-V-C, Estado do Pará, Escala 1:250.000.* Belém; CPRM, (CD-ROM).

Freitas S.C.F. & Klein E.L. 2013. The mineralizing fluid in the Piaba gold deposit, São Luís cratonic fragment (NW-Maranhão, Brazil) based on fluid inclusion studies on quartz veins. *Brazilian Journal of Geology*, **43**:70-84.

Goldfarb R.J., Baker T., Dubé B., Groves D.I., Hart C.J., Gosselin P. 2005. Distribution, character, and genesis of gold deposits in metamorphic terranes. *Economic Geology*, 100th anniversary volume, p. 407-450.

Groves D.I., Goldfarb R.J., Robert F., Hart C.J.R. 2003. Gold deposits in metamorphic belts: overview of current understanding, outstanding problems, future research, and exploration significance. *Economic Geology*, **98**:1-29.

Klein E.L. & Koppe J.C. 2000. Chlorite geothermometry and physicochemical conditions of gold mineralization in the Paleoproterozoic Caxias deposit, São Luís Craton, northern Brazil. *Geochimica Brasiliensis*, **14**:219-232.

Klein E.L. & Moura C.A.V. 2008. São Luís craton and Gurupi belt (Brazil): possible links with the West-African craton and surrounding Pan-African belts. *In:* Pankhurst R.J., Trouw R.A.J., Brito Neves B.B., de Wit M.J. (eds.), West Gondwana: Pre-Cenozoic Correlations across the South Atlantic Region. Geological Society of London, Special Publication, n. 294, p. 137-151.

Klein E.L. & Sousa C.S. 2012. *Geologia e recursos minerais do Estado do Maranhão. Texto explicativo do mapa geológico e de recursos minerais do Estado do Maranhão, escala 1:750.000.* Belém: CPRM, 149 p.

Klein E.L., Fuzikawa K., Koppe J.C. 2000. Fluid inclusion studies on Caxias and Areal gold mineralizations, São Luís Craton, northern Brazil. *Journal of Geochemical Exploration,* **71**:51-72.

Klein E.L., Koppe J.C., Moura C.A.V. 2002. Geology and geochemistry of the Caxias gold deposit, and geochronology of the gold-hosting Caxias Microtonalite, São Luís Craton, northern Brazil. *Journal of South American Earth Sciences,* **14**:837-849.

Klein E.L., Moura C.A.V., Pinheiro B.L.S. 2005a. Paleoproterozóic crustal evolution of the São Luís Craton, Brazil: evidence from zircon geochronology and Sm-Nd isotopes. *Gondwana Research,* **8**:177-186.

Klein E.L., Moura C.A.V., Harris C., Giret A. 2005b. Reconnaissance stable isotope (C, O, H, S) study of Paleoproterozoic gold deposits of the São Luis Craton and country rocks, Northern Brazil: implications for gold metallogeny. *International Geology Review,* **47**:1131-1143.

Klein E.L., Larizzatti J.H., Marinho P.A.C., Rosa-Costa L.T., Luzardo R., Faraco M.T.L. 2008a. *Geologia e recursos minerais da Folha Cândido Mendes, Estado do Maranhão, Escala 1:100.000.* Belém: CPRM-Serviço Geológico do Brasil, 146 p.

Klein E.L., Luzardo R., Moura C.A.V., Armstrong, R. 2008b. Geochemistry and zircon geochronology of paleoproterozoic granitoids: further evidence on the magmatic and crustal evolution of the São Luís cratonic fragment, Brazil. *Precambrian Research,* **165**:221-242.

Klein E.L., Luzardo R., Moura C.A.V., Lobato D.C., Brito R.S.C., Armstrong R. 2009. Geochronology, Nd isotopes and reconnaissance geochemistry of volcanic and metavolcanic rocks of the São Luís Craton, northern Brazil: implications for tectonic setting and crustal evolution. *Journal of South American Earth Sciences,* **27**:129-145.

Klein E.L., Rodrigues J.B., Lopes E.C.S., Soledade G.L. 2012. Diversity of Rhyacian granitoids in the basement of the Neoproterozoic-Early Cambrian Gurupi Belt, northern Brazil: geochemistry, U-Pb zircon geochronology, and Nd isotope constraints on the Paleoproterozoic magmatic and crustal evolution. *Precambrian Research,* **220-221**:192-216.

Klein E.L., Lucas F.R.A., Queiroz J.D.S., Freitas S.C.F., Renac C., Galarza M.A., Jourdan F., Armstrong R. Metallogenesis of the Paleoproterozoic Piaba orogenic gold deposit, São Luís cratonic fragment, Brazil (in review).

Kober B. 1986. Whole grain evaporation for [207]Pb/[206]Pb age investigations on single zircons using a double filament source. *Contributions to Mineralogy and Petrology,* **93**:482-490.

Kuiper K.F., Deino A., Hilgen F.J., Krijgsman W., Renne P.R., Wijbrans J.R. 2008. Synchronizing rock clocks of earth history. *Science,* **320**:500-504.

Ludwig K.R. 2003. User's manual for Isoplot/Ex Version 3.00 – A geochronology toolkit for Microsoft Excel. Berkeley Geochronological Center, Special Publication 4, p. 70.

Moura P. 1936. Ouro no Gurupy. *Mineração e Metallurgia,* **1**:9-13.

Palheta E.S., Abreu F.A.M., Moura C.A.V. 2009. Granitóides proterozóicos como marcadores da evolução geotectônica da região nordeste do Pará – Brasil. *Revista Brasileira de Geociências,* **39**:647-657.

Pastana J.M.N. 1995. *Programa Levantamentos Geológicos Básicos do Brasil. Programa Grande Carajás. Turiaçu/Pinheiro, folhas SA.23-V-D/SA.23-Y-B. Estados do Pará e Maranhão, Escala 1:250.000.* Brasília: CPRM, 205 p.

Perrouty S., Allières L., Jessell M.W., Baratoux L., Bourassa Y., Crawford B. 2012. Revised Eburnean geodynamic evolution of the gold-rich southern Ashanti Belt, Ghana, with new field and geophysical evidence of pre-Tarkwaian deformations. *Precambrian Research,* **204-205**:12-39.

Rodrigues E.M.S. 1992. Implantação do Método Pb-Pb em Rochas Totais. Exemplos de Aplicação em Rochas da Província Mineral de Carajás. Dissertação de Mestrado, Universidade Federal do Pará, p. 128.

Stacey J.S. & Kramers J.D. 1975. Approximation of terrestrial lead isotope evolution by a two-stage model. *Earth Planetary Science Letters,* **26**:207-221.

Vasconcelos P.M., Onoe A.T., Kawashita K., Soares A.J., Teixeira W. 2002. [40]Ar/[39]Ar geochronology at the Instituto de Geociências, USP: instrumentation analytical procedures and calibration. *Anais da Academia Brasileira de Ciências,* **74**:297-342.

Vavra G. 1994. Systematics of internal zircon morphology in major Variscan granitoid types. *Contributions to Mineralogy and Petrology,* **117**: 331-344

Williams I.S. 1998. U-Th-Pb geochronology by ion microprobe. *In*: McKibben M.A., Shanks W.C., Ridley W.I. (eds.), *Applications of Microanalytical Techniques to Understanding Mineralizing Processes.* Reviews in Economic Geology, **7**: 1-35.

Arquivo digital disponível on-line no site www.sbgeo.org.br